

Chiral Diphosphine ddppm-Iridium Complexes: Effective Asymmetric Imine Hydrogenations at Ambient Pressures

Athanasia Dervisi,* Cristina Carcedo, Li-ling Ooi

School of Chemistry, Cardiff University, Main Building, Park Place, Cardiff, CF10 3AT, UK
Phone: (+44)-29-2087-4081, fax: (+44)-29-2087-4030, e-mail: dervisia@cf.ac.uk

Received: July 14, 2005; Accepted: October 20, 2005

Abstract: Complexes of the type $[\text{Ir}(\text{ddppm})(\text{COD})]\text{X}$ were prepared and tested in the asymmetric hydrogenation of a range of imine substrates. Contrary to known iridium catalysts, the ddppm complexes formed efficient catalysts under an atmospheric hydrogen pressure, whereas at higher pressures the catalytic activity of the system was drastically reduced. Depending upon the reaction conditions, *N*-aryl-imines, $\text{Ar}'\text{N}=\text{CMeAr}$, were hydrogenated to the corresponding secondary amines in high yields and enantioselectivities (80–94% ee). In contrast to the $[\text{BF}_4]^-$ and $[\text{PF}_6]^-$ complexes, coordinating anions such as

chloride did not form active Ir-ddppm hydrogenation catalysts. The cationic Ir-ddppm hydrogenation system performed well in chlorinated solvents, whereas coordinating solvents deactivated the system. Dimeric and trimeric Ir(III) polyhydride complexes were formed from the reaction of $[\text{Ir}(\text{ddppm})(\text{COD})]\text{PF}_6$ with molecular hydrogen at atmospheric pressure and were found to inhibit catalytic activity.

Keywords: amines; asymmetric hydrogenation; diphosphane ligands; imines; iridium; iridium hydrides

Introduction

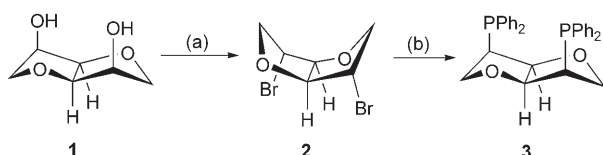
The synthesis of non-racemic chiral amines is of central importance in many aspects of chemistry and biology. The preparation of amines often necessitates the tedious resolution of racemic amines, which is both laborious and atom inefficient and thus there is a general need for efficient alternative routes to chiral amines that utilise readily available precursors. Chiral aromatic amines are particularly sought after due to applications in the pharmaceutical, agrochemical and fine chemical industries. In this respect, metal-catalysed asymmetric reductions of imines have attracted much interest in the last decade and have been the subject of several studies.^[1]

Ruthenium- and rhodium-based catalytic systems are excellent in hydrogenating functionalised olefins and ketones but are much less efficient with imine substrates, with the notable exception of imine transfer hydrogenations.^[2] Iridium hydrogenation catalysts, on the other hand, will reduce substrates which are difficult to hydrogenate, such as imines^[1,3] and sterically crowded, non-functionalised olefins.^[4] Several iridium catalysts have been reported that afford good enantioselectivities in imine reduction, but in order to achieve reasonable hydrogenation rates high pressures of H_2 are required, typically 25–100 bar. An iridium-diphosphine catalyst based on a binaphthyl backbone has been reported by

Zhang et al. with very high enantioselectivities.^[1j] The Ir-ferrocenyl-diphosphine system, developed by Blaser et al., achieved high reaction rates ($\text{TOF} \sim 2800 \text{ h}^{-1}$) with good enantioselectivity (79% ee).^[5,6] This catalyst is used industrially for the synthesis of a key intermediate to the herbicide (*S*)-Metolachlor. Pfaltz et al. have used a phosphino-oxazoline system obtaining up to 89% ee.^[1m] More recently, de Vries' group reported the development of a chiral monodentate phosphinite-Ir catalyst,^[1g] using pyridine as an additive raised the ee to 83% at 25 bar. Phosphite- and phosphonite-based iridium catalysts however, did not induce enantioselectivity in imine hydrogenations.^[1k]

Despite the above advances, iridium imine hydrogenations are still underdeveloped when compared to the state of the art in alkene hydrogenation chemistry. The main obstacles that need to be overcome are the normally high operating hydrogen pressures, the moderate enantioselectivities usually obtained, the limited range of imines hydrogenated and the catalyst stability.

Recently, we reported in a communication the synthesis of the *endo*-diphosphine ddppm (**3**) and preliminary results from the hydrogenation of alkenes with Rh and Ru ddppm-based catalysts.^[7] As shown in Scheme 1, ddppm is prepared from the commercially available dehydroxitol (**1**) after short syntheses. Here, we give an account of our studies on the hydroge-

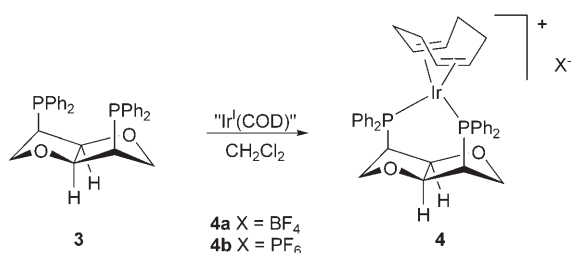


Scheme 1. (a) 2 equivs. of $\text{Br}_2/\text{PPh}_3/\text{imidazole}$, CH_3CN , reflux; (b) 2 equivs. of LiPPh_2 , Et_2O .

nation of prochiral imines with cationic iridium-ddppm catalytic system and Discussion

Synthesis and Structure of the Cationic Iridium-ddppm Complexes **4a** and **b**

Iridium-ddppm complexes of the type $[\text{Ir}(\text{ddppm})\text{-(COD)}]\text{X}$, where $\text{X} = \text{BF}_4$ or PF_6 , were prepared according to Scheme 2. Attempts in isolating an Ir-ddppm chloride complex from the reaction of $[\text{Ir}(\text{COD})\text{Cl}]_2$ with ddppm did not afford a distinct complex.



Scheme 2. Synthesis of the iridium complexes **4a** and **4b**.

Reaction of $[\text{Ir}(\text{COD})_2]\text{BF}_4$ with one equivalent of ddppm under an inert atmosphere formed the cationic complex $[\text{Ir}(\text{ddppm})(\text{COD})]\text{BF}_4$ (**4a**) in quantitative yield. The $^{31}\text{P}\{^1\text{H}\}$ NMR spectrum of **4a** reveals a singlet at $\delta = 15.2$. In the ^1H NMR spectrum complex **4a** shows four unresolved multiplets in 1:1:1:1 ratio for the ddppm protons at $\delta = 3.98$, 4.12, 4.24 and 5.38 ppm. The most characteristic ^1H NMR shifts for ddppm upon coordination are those of the CH protons. The resonance for the bridgehead CH protons shifts from $\delta = 2.94$ ppm in the free ligand to $\delta = 3.98$ in the iridium complex. Similarly, the methine CHP protons shift from $\delta = 4.52$ to 5.38. Two signals were observed for the olefinic protons of the 1,5-COD ligand, consistent with the C_2 symmetric environment, at $\delta = 3.53$ and 4.32.

The hexafluorophosphate derivative $[\text{Ir}(\text{ddppm})(\text{COD})]\text{PF}_6$ (**4b**) was prepared from the reaction of ddppm with $[\text{Ir}(\text{COD})\text{Cl}]_2$ and NH_4PF_6 following a previously reported protocol.^[11] NMR spectroscopic data were identical with the ones for the BF_4^- complex. The Ir(I) complexes **4a** and **4b** are air-stable and thus easier to handle than their rhodium analogues,

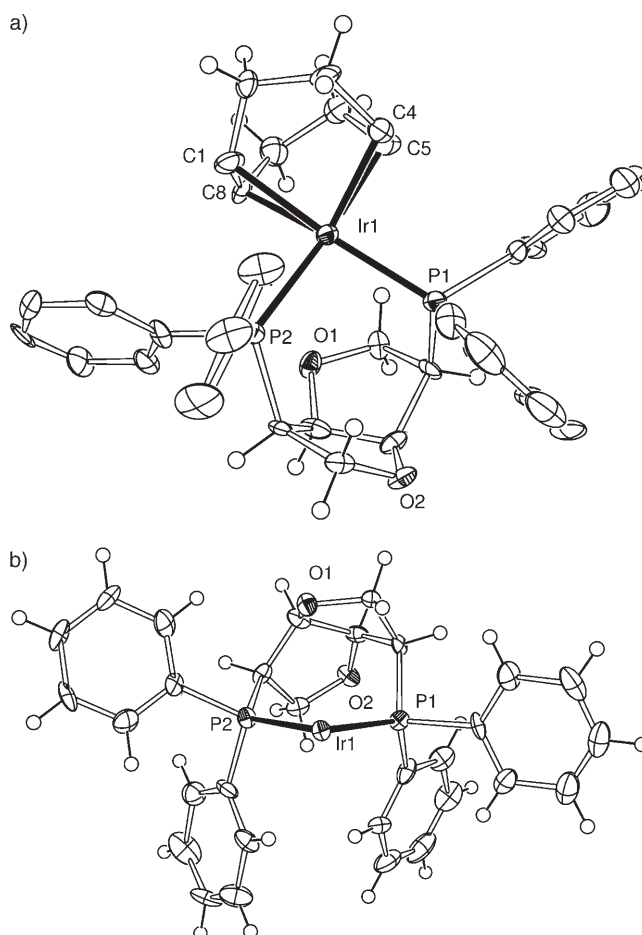


Figure 1. ORTEP-3^[8] representations of complex **4a**. The BF_4 anion and part of the hydrogen atoms on the aromatic rings and COD have been omitted for clarity. In the second drawing, only the $\text{Ir}(\text{ddppm})$ fragment of **4a** is shown.

$[\text{Rh}(\text{ddppm})(\text{COD})]\text{X}$, which show moderate stability under aerobic conditions.^[7]

Needle-shaped red crystals of the iridium complex $[\text{Ir}(\text{ddppm})(\text{COD})]\text{BF}_4$ grown from slow diffusion of ether into a dichloromethane solution were used in the crystal structure determination of **4a**. Structural representations of **4a** are given in Figure 1, showing the ddppm ligand chelating to the metal centre. Of note is the nearly eclipsed conformation of the two PPh_2 phenyl groups, shown more clearly in the lower drawing of Figure 1. This orientation of the aromatic rings in **4a** lifts the pseudo- C_2 symmetry, of the M-ddppm fragment, usually observed in the solid state for the ddppm complexes.^[7,9] Such an arrangement although sterically more demanding is not unusual in the solid state for Ir(I)(diphosphine)-COD complexes, and it is attributed to crystal packing effects.^[10,11] The ligand bite angle at $94.50(10)^\circ$ is the smallest observed so far within the range of bidentate complexes with ddppm.^[12] The related $[\text{Rh}(\text{ddppm})(\text{CH}_3\text{CN})_5]\text{BF}_4$ complex has a bidentate angle of $98.61(3)^\circ$.^[7]

Hydrogenation of Imines with Ir-ddppm Catalysts

The new iridium complexes were tested in the asymmetric hydrogenation of a range of aromatic imines. Under the given reaction conditions the cationic iridium complexes **4a** and **4b** afforded *N*-arylamines in high yields and with enantioselectivities at the top of the reported range for this class of compounds. The effect of the hydrogen pressure, solvent and other variables in the yield and selectivity of the reaction were studied and results are presented in the following paragraphs.

Hydrogen Pressure Effect

N-(1-Phenylethylidene)aniline (**5a**) was used as a representative aromatic imine in order to establish the optimum reaction conditions. Table 1 shows the effect of hydrogen pressure in the hydrogenation of imine **5a**, using $[\text{Ir}(\text{COD})(\text{ddppm})][\text{BF}_4]$ as the catalyst precursor. In contrast to previous observations,^[1] increasing the hydrogen pressure led to deactivation of the system, with best results obtained under an atmospheric pressure of hydrogen gas. Increasing the hydrogen pressure to 4 bar resulted in a small increase in imine formation from 68 to 72%. However, this was followed by an appreciable drop in enantioselectivity from 80 to 73% ee (entries 1 and 2). A positive effect on enantioselectivity at lower hydrogen pressures has been observed previously, although within a broader range of hydrogen pressures (20–50 bar).^[1c,4a] Further increase of the hydrogen pressure to 10 bar resulted in virtually complete deactivation of the catalyst. Finally, at 45 bar of hydrogen pressure only a slight increase in the yield was observed, at 14%.

Iridium hydrogenation reactions usually take place within the range of 20–100 bar due to the adverse effect of low H_2 pressure on the reaction rate which, in many cases, leads to complete catalyst deactivation.^[1c, h, 13] Indeed, kinetic studies with the $[\text{Ir}(\text{COD})(\text{PPh}_3)_2][\text{PF}_6]$ precatalyst show a linear increase in the reaction rate with increasing hydrogen pressure.^[3] The loss of activity of the Ir-ddppm system at higher hydrogen pressures may be attributed to the predominance of inactive iridium-polyhydride clusters at elevated pressures. Formation of unreactive Ir–H complexes is also supported by the results of entry 5 (Table 1), where saturation of the catalyst solution with hydrogen gas before addition of the substrate produced a practically inactive catalyst affording the corresponding amine in very low yield (5%). The Ir(III) hydride species formed have been characterised and their properties are discussed in a later section.

Solvent/Catalyst Precursor Effects

The ability of the Ir-ddppm system to operate at atmospheric H_2 pressures allowed us to carry out the following

Table 1. Effect of the H_2 pressure in the asymmetric hydrogenation of imine **5a**.^[a]

Entry	$P(\text{H}_2)$ bar	Yield [%]	ee [%]
1	1	68	80
2	4	72	73
3 ^[b]	10	< 5	–
4 ^[b]	45	14	–
5 ^[b]	4	5 ^[a]	–

Reaction conditions: 0.01 mmol $[\text{Ir}(\text{COD})(\text{ddppm})]\text{BF}_4$, 1 mmol substrate in 5 mL of CH_2Cl_2 , at room temperature, 24 h.

^[a] Catalyst solution saturated with hydrogen before addition of imine **5a**.

^[b] The ee (%) was not determined.

hydrogenation reactions using conventional Schlenk techniques without the need for high-pressure apparatus. Table 2 shows the effect of different solvents and catalyst precursors in the hydrogenation of imine **5a**. In 1,2-dichloroethane (entry 1) $[\text{Ir}(\text{COD})(\text{ddppm})][\text{PF}_6]$ afforded amine **5b** in quantitative yield with 84% enantioselectivity compared to 62% yield and 82% ee with the BF_4^- precursor **4a** (entry 2). In CH_2Cl_2 comparable yields and enantioselectivities were obtained with **4a** (entry 3). Other weakly co-ordinating solvents such as toluene were much less effective affording both very low yields and selectivities. In co-ordinating solvents such as methanol a low yield was obtained (20%) but with higher enantioselectivity at 89% ee. In THF the catalyst was almost inactive and less than 5% of conversion to the secondary amine was obtained. A similar solvent dependence has been reported for the cationic Ir(I)-COD systems with triphenylphosphine^[3] and phosphino-oxazoline ligands.^[1c, m, 14] A catalytic run with the $[\text{Ir}(\text{COD})\text{Cl}]_2/\text{ddppm}$ system in dichloromethane (entry 7) showed negligible activity in imine reduction. This is in contrast to other diphosphine-based Ir catalysts which perform better with neutral precursors ($[\text{Ir}(\text{COD})\text{Cl}]_2/\text{diphosphine}$).^[1a, j, h, m, 5, 6, 15] The above results show that the activity of the Ir-ddppm system is increased dramatically in non-co-ordinating solvents and with cationic precursors bearing weakly co-ordinating anions (in increasing order: Cl^- , BF_4^- , PF_6^-). Pfaltz et al. have reported a similar counterion dependence with iridium catalysts, where the more bulky and weakly co-ordinating anions formed better catalysts.^[4a] Contrary to literature reports, hydrogenation reactions with additives such as molecular sieves, trifluoroacetic acid, methanol or tetrabutylammonium iodide gave low yields and significant amounts of hydrolysis products.^[6, 13a, 15]

Table 2. Effect of the solvent and catalyst precursor in the asymmetric hydrogenation of imine **5a**.

Entry	Solvent	Catalyst	Yield [%] ^[a]	ee (<i>R</i>) [%]
1	(CH ₂ Cl) ₂	4b	100	84
2	(CH ₂ Cl) ₂	4a	62	82
3	CH ₂ Cl ₂	4a	68	80
4	CH ₃ OH	4a	20	89
5 ^[b]	THF	4a	< 5	–
6 ^[b]	PhCH ₃	4a	7	–
7 ^[b]	CH ₂ Cl ₂	[Ir(COD)Cl] ₂ /ddppm	< 5	–

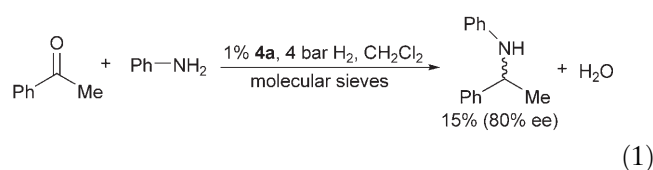
Reaction conditions: 0.01 mmol of catalyst precursor, 1 mmol substrate in 5 mL of solvent, atmospheric H₂ pressure, at room temperature, 24 h. % ee values were measured by chiral HPLC using a Chiralcel OD column and hexane/IPA as the eluent.

^[a] Determined by NMR.

^[b] The ee (%) was not determined.

After determining the optimum reaction conditions with *N*-phenylimine (**5a**) a number of imine substrates were tested in order to establish the range of imines hydrogenated by the Ir-ddppm system. The imines shown in Table 3 were hydrogenated in dichloroethane under an atmospheric pressure of hydrogen gas with the [PF₆][–] catalyst precursor **4b**. *N*-Arylimines were hydrogenated quantitatively to the corresponding amine with enantioselectivities between 80 and 94%. A clear correlation between enantioselectivity and the electronic properties of *para*-substituents was not observed. The *N*-anisylimine **8a** gave the best enantioselectivity within the series. Hydrogenation of **8a** was of interest due to the ease of conversion into the primary amine.^[11] Lower catalyst loadings were also tested with the hydrogenation of **8a**. At 0.5 mol % of the catalyst close to quantitative yields were obtained with 93% ee (entry 5); further lowering of the catalyst resulted in incomplete reaction. Reactions were normally run for 24 hours without monitoring. When the hydrogenation of imine **8a** was followed it was found that after 6 hours the amine was formed in 70% yield and 90% enantioselectivity; the reaction reached completion after 9 hours with 94% ee (entry 6). Researchers have reported previously the facile racemisation of *N*-arylamine-iridium complexes *via* C–H activation.^[16] In order to establish whether a similar process takes place with the Ir-ddppm catalyst the hydrogenation of imine **8a** was followed over the course of several days. A slow drop in enantioselectivity from 94 to 88% was observed during the course of 3 days.

N-Benzylimine **9a** was also hydrogenated under the standard conditions and gave the corresponding amine in low yield (20%) and enantioselectivity (5%). Trimethylindolenine imine, **10a**, remained unreacted under the same reaction conditions. During hydrogenation of **10a** a characteristic pale yellow solution, which indicates formation of the Ir–H catalyst, was not observed.^[15] Thus leading us to attribute the absence of any activity with imine **10a** to the formation of a stable Ir-imine complex.



Since iridium hydrogenation catalysts do not appear to hydrogenate ketonic substrates we hydrogenated directly a mixture of acetophenone and aniline [Eq. (1)].^[3a,5a] NMR analysis after termination of the reaction showed formation of the secondary amine at 15% yield and 80% ee together with equimolar amounts of acetophenone, aniline and the corresponding imine. The low reaction yields observed in this case may be attributed to the competition of acetophenone and aniline with the imine substrate for coordination to the active site of the metal.

Iridium(III)-ddppm Hydride Complexes

Iridium complexes of the type [Ir(COD)L₂]X, where L is a P or N donor ligand, react with hydrogen to form dimeric and trimeric Ir–H clusters analogous to structures **11** and **12**, respectively (Scheme 3).^[17] In the case of phosphino-oxazoline systems such hydride species were found to be inactive in hydrogenation reactions.^[17a]

During hydrogenation experiments with the Ir-ddppm catalyst an immediate colour change was observed when H₂ gas was introduced, from bright red to pale yellow attributed to the formation of Ir-ddppm hydride species. In addition, catalytic activity was inhibited when the catalyst solution was treated with hydrogen gas prior to addition of the imine substrate (Table 1, entry 5). These observations prompted us to study further the reactivity of the Ir-ddppm system with molecular hydrogen. In a typical experiment, a methanol solution of complex **4b** containing a twenty-fold excess of KPF₆ was stirred for one day under an atmosphere of hydrogen. During that period a microcrystalline solid precipitated.

Table 3. Asymmetric hydrogenation of imines catalysed with the iridium complex **4b**.

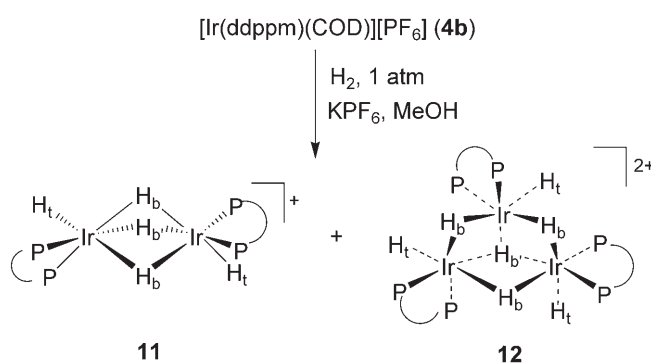
Entry	Substrate	Yield [%]	ee [%] ^[a]
1		99	84% (<i>R</i>)
2		99	80 (–)
3		100	81 (+)
4		100	94 (+)
5 ^[b]		98	93 (+)
6 ^[c]		99	94 (+)
7		20	5 (<i>R</i>)
8		0	–

Reaction conditions: 0.01 mmol [Ir(COD)(ddppm)]PF₆, 1 mmol substrate in 5 mL of (CH₂Cl)₂, at room temperature, run for 24 h unless otherwise stated.

^[a] Determined by chiral HPLC; absolute configurations (or the sign of optical rotation) assigned by comparison of retention times with literature values.

^[b] 0.5% mmol of **4b**.

^[c] Run for 9 hours.

**Scheme 3.** Hydride complexes obtained from the reaction of [Ir(COD)ddppm]PF₆ with H₂ (**11/12** = 3:2).

NMR analysis of the isolated solid showed the formation of the iridium clusters: [Ir₂(ddppm)₂(μ²-H)₃(H)₂]PF₆ (**11**) and [Ir₃(ddppm)₃(μ³-H)(μ²-H)₃(H)₃][PF₆]₂ (**12**), in a 3/2 ratio (Scheme 3). Although attempts to separate the two complexes did not meet with success, by using a variety of one- and two-dimensional NMR techniques, including ¹H-³¹P correlation measurements, their identities were confirmed (Table 4).

The ³¹P NMR signals of **11** at 17.6 and 9.9 ppm are part of an AX system showing a small but unresolved *cis* P–P coupling. Figure 2 shows the ³¹P, ¹H correlation spectrum for complexes **11** and **12**. Dimer **11** displays four cross-peaks in the hydride region arising from ²J_{P,H} interactions. The doublet at δ = –6.54 (²J_{P,H} = 83.6 Hz) arises from the two equivalent bridging hydrides (H_b) *trans* to a single phosphorus atom. The remaining bridging hydride (H_b) resonates as a triplet, due to two *trans* phosphorus atoms, at δ = –8.48 (²J_{P,H} = 67.1 Hz). The observed coupling constants for the bridging iridium hydrides are smaller than the ones reported for terminal hydrides *trans* to phosphorus (120–160 Hz) due to their reduced bond order.^[18,19] The two equivalent terminal hydrides resonate at a significantly lower frequency at δ = –24.42 showing a multiplet with a small coupling constant, ²J_{P,H} ~ 25 Hz, as a result of coupling to two *cis* phosphorus atoms. The ¹H NMR data for dimer **11**, including coupling constants, are in good agreement with those reported for the analogous PPh₃ and dppe^[20] complexes.^[17d, f]

The ³¹P NMR spectrum of trimer **12** reveals two signals at 20.3 and 9.9 ppm showing unresolved *cis* P–P coupling. The correlated hydride resonances appear at

Table 4. NMR data for the iridium-hydride complexes **11** and **12**.^[a]

Complex	δ(³¹ P) ^[b]	Bridging H (² J _{P,H} , Hz)	Terminal H (² J _{P,H} , Hz)
11	17.6; 9.9	–6.54 (d, 83.6, 2H _b); –8.48 (t, 67.1, 1H _b)	–24.42 (m, ~25, 2H _t)
12	20.3; 9.9	–6.88 (d, 92.4, 3H _b); –7.12 (qt, 34.7, 1H _b)	–23.71 (m, ~20, 3H _t)

^[a] In dichloromethane-*d*₂.

^[b] Unresolved multiplets.

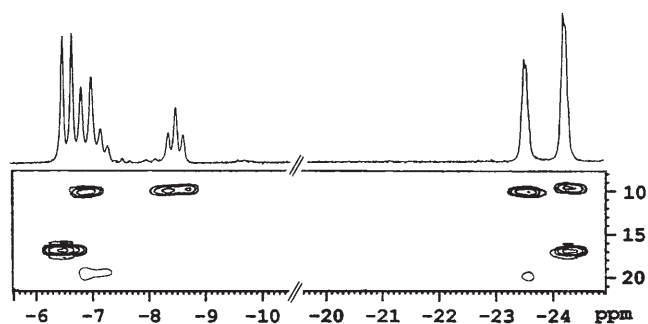


Figure 2. Section of the ^1H , ^{31}P correlation for **11** and **12** showing the three hydride resonances associated with the signals at 17.6 and 9.9 (δ_{P}) for **11** and the hydride cross-peaks owing to complex **12** (correlating with the signals at δ_{P} = 9.9 and 20.3 ppm).

– 6.88 (d, $^2J_{\text{PH}} = 92.4$ Hz), – 7.12 (qt, $^2J_{\text{PH}} = 34.7$ Hz) and – 23.71 (m, $^2J_{\text{PH}} \sim 20$ Hz) ppm, in a 3/1/3 ratio; the two bridging hydride signals at $\delta_{\text{H}} = 6.88$ and 7.12 overlap with each other. The magnitudes of the $^2J_{\text{PH}}$ coupling constants are consistent with their assignment and close to those of other reported Ir–H trimers.^[17a, d] Complexes **11** and **12** were also the only phosphorus species identified after NMR analysis of a typical Ir-ddppm hydrogenation reaction.

The above findings show that the main path of catalyst deactivation for the Ir-ddppm system is *via* formation of unreactive Ir(III) hydride clusters. During the catalytic reactions imine coordination prevents formation of such clusters but as the reaction progresses imine concentration diminishes and formation of the complexes **11** and **12** commences. At higher than atmospheric hydrogen pressures (and consequently higher molecular H_2 concentrations) the imine substrate competes less favourably with molecular hydrogen for binding to the metal leading to rapid catalyst deactivation. The narrower range of H_2 pressures that the Ir-ddppm system operates may be attributed to the weak binding of *N*-aryl imine substrates to the Ir-ddppm catalyst.

Conclusion

We have shown that the cationic iridium-ddppm complexes **4a** and **b** form efficient imine hydrogenation catalysts displaying good to high enantioselectivities without the need to operate at high hydrogen pressures for effective hydrogenation. The catalyst precursors are readily prepared, easily handled and air-stable. In contrast to the cationic complexes **4a** and **b**, the neutral $[\text{Ir}(\text{COD})\text{Cl}]_2$ -ddppm system was inactive in the hydrogenation of imines suggesting that cationic, unsaturated intermediates are preferred with the Ir-ddppm catalyst. This was further supported from the pronounced

effect that different solvents had on the catalyst's activity. Co-ordinating solvents such as THF and methanol effectively deactivated the catalyst, whereas in 1,2-dichloroethane quantitative yields of the secondary amine were obtained. Our results indicate a considerable potential for this class of catalysts especially for hydrogenations under atmospheric pressure, which merit further investigation. Based on our current understanding of the system, the negative effect of hydrogen pressure on the activity and selectivity of the catalyst has been attributed to the formation of inactive iridium(III) hydride clusters. Further work is in progress to address this point.

Experimental Section

General Remarks

All manipulations were performed using standard Schlenk techniques under an argon atmosphere, except where otherwise noted. Complexes **4a** and **4b** after their formation were treated under aerobic conditions. Solvents of analytical grade and deuterated solvents for NMR measurements were distilled from the appropriate drying agents under N_2 immediately prior to use following standard literature methods.^[21] Literature methods were employed for the synthesis of $[\text{Ir}(\text{COD})\text{Cl}]_2$ ^[22] and imines **5a**,^[1m] **6a**,^[ii] **7a**,^[ii] **8a**^[ii] and **9a**.^[1m] All other reagents were used as received.

Microanalyses were obtained from Warwick analytical service Ltd. Where reproducible microanalyses could not be obtained the NMR spectra of the samples suggested their purity was greater than 95%. NMR spectra were obtained on Bruker Avance AMX 400, 500 or Jeol Eclipse 300 spectrometers and referenced to external TMS. HPLC analyses were performed on an Agilent 1100 series instrument. Mass spectra were obtained in the ES (electrospray) mode unless otherwise reported from the EPSRC Mass Spectrometry Service, Swansea University. High-resolution mass spectra (ES) were recorded in house on a Waters Q-Tof micromass spectrometer.

Preparation of 1,4:3,6-Dianhydro-2,5-dideoxy-2,5-dibromo-L-itol (2)

A 500-mL flask was charged with triphenylphosphine (23 g, 86 mmol) under argon followed by the addition of dry acetonitrile (150 mL). To the resulting solution bromine (90 mmol) was added dropwise at 0 °C. Subsequently an acetonitrile solution of imidazole (5.6 g, 82 mmol) and isomannide (6 g, 41 mmol) were transferred to the flask. The reaction mixture was refluxed for 2 days. The mixture was cooled in an ice bath and any precipitate formed was filtered and the filtrate concentrated to *ca.* 50 mL. The filtrate was then absorbed onto a silica column (15 × 6 cm) and eluted with a petroleum ether/ethyl acetate (9:1) mixture. Pooling of fractions and solvent evaporation afforded compound **2** ($R_f = 0.30$). 1,4:3,6-Dianhydro-2,5-dideoxy-2,5-dibromo-L-itol was obtained as colourless crystals after recrystallisation from either hot ethanol or petroleum ether; yield: 9.15 g (83%). The above is an im-

proved procedure for compound **2**; spectroscopic data are available in the literature.^[23]

1,4:3,6-Dianhydro-2,5-bis(diphenylphosphino)-D-mannitol (ddppm)

Diphenylphosphine (3.3 mL, 19.1 mmol) was syringed into ether (30 mL) at 0 °C and subsequently *n*-BuLi (1.71 M, 11.2 mL) was added. After 30 minutes an ether solution of **2** (2.6 g, 9.6 mmol) was added dropwise to the stirred reaction mixture. The yellow solution was allowed to slowly warm to room temperature and stirred until the solution became colourless with the precipitation of a heavy white precipitate. Degassed water (15 mL) was added and the ether layer separated. The water layer successively was washed with ether (2 × 20 mL) and the ether extracts collected. Evaporation of the solvent under vacuum afforded ddppm as an air-stable white microcrystalline solid. Recrystallisation from hot ethanol afforded the title compound as colourless needles; yield: 0.67 g (52%). ¹H NMR (400 MHz, CDCl₃): δ = 2.94 (m, 2H, CHPh₂), 3.88 (m, 4H, CH₂), 4.52 (m, 2H, CCH), 7.2–7.4 (m, 20H); ³¹P NMR (75 MHz, CDCl₃): δ = –21.4 (s); ¹³C NMR (100 MHz, CDCl₃): δ = 45.78 (d, *J*_{C,P} = 11.5 Hz, 2C), 73.04 (d, *J*_{C,P} = 26.5 Hz, 2C), 86.12 (m, 2C), 128.63 (s, 2C, Ar), 128.65 (m, 2C, Ar), 129.03 (m, 2C, Ar), 133.04 (d, *J*_{C,P} = 19.6 Hz, 2C, Ar), 133.51 (d, *J*_{C,P} = 21.4 Hz, 2C, Ar), 136.69 (d, *J*_{C,P} = 13.3 Hz, 1C, Ar), 137.44 (d, *J*_{C,P} = 15.0 Hz, 1C, Ar); MS (accurate mass, ES⁺): *m/z* (%), calculated mass for [M + H]⁺: 483.1637, measured: 483.1636; elemental analysis calcd. (%) for C₃₀H₂₈O₂P₂ (482.5): C 74.68, H 5.85; found: C 73.82, H 5.57.

[Ir(COD)₂]BF₄

To a dichloromethane solution (2 mL) of [Ir(COD)Cl]₂ (0.135 g, 0.2 mmol) and 1,5-cyclooctadiene (0.5 mL, 4.07 mmol, previously purified by passing through a short silica column) AgBF₄ (92.5 mg, 0.475 mmol) was added. The resulting deep red slurry was stirred in the dark for 1.5 hours, subsequently filtered through celite and washed with CH₂Cl₂ (2 mL). The solution was concentrated and anhydrous Et₂O (15 mL) was added to precipitate the complex. The red solid formed was filtered, washed with cold Et₂O (3 × 10 mL) and dried; yield: 0.18, (91%). ¹H NMR (CDCl₃, 250 MHz): δ = 2.43 (m, 8H, CH₂), 5.18 (m, 4H, CH); ¹³C NMR (100 MHz, CDCl₃): δ = 30.55 (s, CH₂), 100.09 (s, CH).

[Ir(COD)(ddppm)]BF₄ (**4a**)

To a solution of [Ir(COD)₂]BF₄ (103 mg, 0.207 mmol) in dichloromethane ddppm (100 mg, 0.207 mmol) was added. The reaction mixture was left stirring for 1 h after which the solvent was evaporated under vacuum. The resulting bright red solid was washed twice with ether (20 mL) and dried; yield: 154 mg (86%). Deep red crystals of **4a** were obtained after slow diffusion of ether into a chloroform solution. ¹H NMR (400 MHz, CDCl₃): δ = 1.67 (m, 2H, H₂C_{COD}), 2.07 (m, 4H, H₂C_{COD}), 2.32 (m, 2H, H₂C_{COD}), 3.53 (m, 2H, HC_{COD}), 3.98 (m, 2H, CHPh₂), 4.12 (m, 2H, CH₂), 4.24 (m, 2H, CH₂), 4.32 (m, 2H, HC_{COD}), 5.38 (m, 2H, CCH), 7.2–7.5 (m, 20H); ¹³C NMR (100 MHz, CDCl₃): δ = 28.48 (s, H₂C_{COD}), 34.70 (s, H₂

C_{COD}), 45.15 (m, 2C, CH₂), 74.99 (m, 2C, CHP), 83.71 (m, 2C, CHP), 84.33 (s, HC_{COD}), 88.18 (s, HC_{COD}), 128.77 (m, 4C, Ar), 129.53 (m, 4C, Ar), 131.66 (s, 2C, Ar), 132.03 (s, 2C, Ar), 133.94 (m, 4C, Ar), 134.17 (m, 4C, Ar); ³¹P NMR (121 MHz, CDCl₃): δ = 15.3; MS (accurate mass, ES⁺): *m/z* (%), calculated mass for [M – BF₄]⁺: 783.2127; measured: 783.2130; 675.2 (25) [M – BF₄ – COD]⁺; elemental analysis calcd. (%) for C₃₈H₄₀BF₄IrO₂P₂ (869.7): C 52.48, H 4.64; found: C 52.53, H 4.59.

[Ir(COD)(ddppm)]PF₆ (**4b**)

Ddppm (96 mg, 0.2 mmol) and [Ir(COD)Cl]₂ (67 mg, 0.1 mmol) were stirred for two hours in CH₂Cl₂ (5 mL) [δ_P (CH₂Cl₂, 121 MHz): –21.0 (broad), 18.0 (m)]. The resulting orange solution was washed with an aqueous solution of NH₄PF₆ (0.4 M, 5 mL). Subsequently the bright red dichloromethane layer was collected, washed with water and dried over MgSO₄. Filtration of the MgSO₄ and evaporation of the volatiles afforded a red solid. Complex **4b** was isolated in 88% yield (163 mg) after column chromatography using CH₂Cl₂/MeOH (99:1) as the eluent (R_f = 0.2). ³¹P NMR (121 MHz, CDCl₃): δ = 15.3 (s, ddppm), –143.8 (septet, PF₆). All other NMR data were identical to those of complex **4a**.

Reaction of **4b** with H₂

A solution of [Ir(COD)(ddppm)]PF₆ (45 mg, 0.05 mmol) and NH₄PF₆ (163 mg, 1.00 mmol) in 2 mL of dry methanol was stirred under an atmospheric pressure of hydrogen for one hour. Subsequently the vessel was isolated and left stirring further for one day. During the course of the reaction a yellow microcrystalline powder precipitated. The formed solid was collected *via* filtration, washed with Et₂O (2 × 5 mL) and dried under vacuum. NMR analyses showed the formation of complexes **11** and **12**.

Data for complex 11: ¹H NMR (500 MHz, CDCl₃): δ = –24.42 (m, ²*J*_{PH} ~ 25 Hz, 2H, H_i), –8.48 (t, ²*J*_{PH} = 67.1 Hz, 1H, H_b), –6.54 (d, ²*J*_{PH} = 83.6 Hz, 2H, H_b), 3.0–4.1 (m, 6H), 5.24 (m, 2H, CCH), 6.4–8.5 (m, 20H, ArH); ¹³C NMR (125 MHz, CDCl₃): δ = 43.7 (m, 2C, CH₂), 73.8 (m, 2C, CHP), 84.2 (m, 2C, CHP), 128.5 (m, 4C, Ar), 131.1 (m, 2C, Ar), 133.4–134.5 (m, 6C, Ar); ³¹P NMR (121 MHz, CDCl₃): δ = 9.9 (m), 17.6 (m); IR (KBr): ν = 2215 br, m (Ir–H), 1966, 1889, 1810 cm^{–1} br, w (Ir–H); MS (ES⁺): *m/z* (%), [M – PF₆]⁺ = 1353.58 (100.0%); MS (accurate mass, ES⁺) *m/z* (%), calculated mass for [M – (H + PF₆)]²⁺: 676.1339; measured: 676.1325.

Data for complex 12: ¹H NMR (500 MHz, CDCl₃): δ = –23.71 (m, ²*J*_{PH} ~ 20 Hz, 3H, H_i), –7.12 (qt, ²*J*_{PH} = 35 Hz, 1H, H_b), –6.88 (d, ²*J*_{PH} = 92.4 Hz, 3H, H_b), 3.0–4.1 (m, 6H), 5.24 (m, 2H, CCH), 6.4–8.5 (m, 20H, ArH); ³¹P NMR (121 MHz, CDCl₃): δ = 9.9 (m), 20.3 (m).

Typical Hydrogenation Protocol

A Schlenk (50 mL) was charged with *N*-(1-phenylethylidene)aniline **5a** (195 mg, 1 mmol), [Ir(ddppm)(COD)]BF₄ (9 mg, 0.01 mmol) and (CH₂Cl₂)₂ (5 mL) under an N₂ atmosphere. The resulting red solution was placed under partial vac-

uum. Subsequently, hydrogen gas was introduced to the vessel, causing an immediate colour change of the solution to pale yellow. The reaction mixture was stirred under an atmospheric pressure of hydrogen for 24 h, at room temperature. Solvents were removed under vacuum and the % conversion was determined by NMR. The crude product was dissolved in hexane/ether (1:1) and passed through a short plug of silica. Pure *N*-(1-phenylethyl)aniline **5b** can be obtained from a silica column (hexane/2-propanol, 9:1, $R_f=0.38$). % ees were calculated based on chiral HPLC analysis (Daicel Chiralcel OD, 250 × 4.6 mm, $\lambda_{\text{detector}}=220$ nm, flow rate=0.5 mL/min hexane/2-propanol (9:1, v/v); $t_R=12.1$ min (*S*, minor), $t_R=14.2$ min (*R*, major).

(-)-*N*-[1-(4-Chlorophenyl)ethyl]benzenamine (**6b**): HPLC analysis: Chiralcel OD, 1.0 mL/min, *n*-hexane/2-propanol (99:1, v/v), $t_R=16.8$ min (minor), 18.8 min (major).

(+)-*N*-[1-(4-methoxyphenyl)ethyl]benzenamine (**7b**): HPLC analysis: Chiralcel OJ, 1.0 mL/min, *n*-hexane/2-propanol (97:3, v/v), $t_R=45.6$ min (major), 52.0 min (minor).

(+)-4-Methoxy-*N*-(1-phenylethyl)benzenamine (**8b**): the product was passed through a column using CH_2Cl_2 as eluent prior to HPLC analysis due to overlap of the signals of the parent imine with the first eluted isomer of **8b**. HPLC analysis: Chiralcel OD, 0.75 mL/min, *n*-hexane/2-propanol (99:1, v/v), $t_R=21.8$ min (major), 24.3 min (minor).

(*R*)-*N*-Benzyl-1-phenylethanamine (**9b**): the product was passed through a column using CH_2Cl_2 as eluent prior to HPLC analysis. HPLC analysis: Chiralcel OJ, 0.75 mL/min, *n*-hexane/2-propanol (99:1, v/v), $t_R=21.2$ min (minor), 23.3 min (major).

Physical and spectroscopic data for the amines **5b–9b** were in agreement with values reported in the literature. Absolute configurations or the sign of optical rotation were assigned by comparison of the retention times with literature values.^[1c, i, m, 15b]

rac-*N*-(1-Phenylethyl)benzylamine (**5b**)

N-(1-Phenylethylidene)aniline (0.1 g, 0.5 mmol) was dissolved in THF (1 mL) followed by the addition of zinc borohydride (1 mL, 0.5 M).^[24] A colour change was observed from yellow-orange to green and the resulting mixture was stirred overnight under N_2 . The reaction was quenched by careful addition of water until no further evolution of gas was observed. After extraction with ether (3 × 20 mL) the organic layers were combined, washed with brine and dried over Na_2SO_4 . Amine **5b** was obtained after Kugelrohr distillation as a colourless oil; yield: 0.05 g (55%).

Crystal Structure Determination of **4a**

Data collection was carried out on a Bruker-Nonius Kappa CCD diffractometer using graphite monochromated Mo $K\alpha$ radiation. The instrument was equipped with an Oxford Cryo-systems cooling apparatus. The structure was solved *via* Patterson methods (Dirdif 99.2)^[25] and refined on F_o ^[25] by full matrix least squares^[26] using all unique data corrected for Lorentz and polarisation factors and for absorption using SORTAV.^[27] All non-hydrogen atoms were refined anisotropically, while the hydrogen atoms were inserted in idealised positions with

Uiso set at 1.2 or 1.5 times the Ueq of the parent atom. In the final cycles of refinement, a weighting scheme that gave a relatively flat analysis of variance was introduced and refinement continued until convergence was reached.

Crystal data for complex 4a: $\text{C}_{39}\text{H}_{37}\text{Cl}_3\text{Ir}_1\text{O}_2\text{P}_2$, B_1F_4 , $M=984.99$, orthorhombic, space group $P2_12_12_1$, $a=10.4744(4)$, $b=18.1714(7)$, $c=19.9436(7)$ Å, $V=3796.0(2)$ Å³, $Z=4$, $D=1.724$ g cm⁻³, $\mu(\text{Mo-K}\alpha)=3.868$ mm⁻¹, $F(000)=1944$, $T=150(2)$ K, red needles, crystal size 0.05 × 0.05 × 0.25 mm; 6545 independent measured reflections, F^2 refinement, $R_1=0.0572$, $wR_2=0.1183$, 5617 independent observed absorption corrected reflections [$|F_o| > 2\sigma(|F_o|)$, $2\theta_{\text{max}}=50.22^\circ$], 464 parameters, 0 restraints.

CCDC-268684 contains the supplementary crystallographic data for complex **4a**. These data can be obtained free of charge *via* www.ccdc.cam.ac.uk/conts/retrieving.html (or from the Cambridge Crystallographic Data Centre, 12 Union Road, Cambridge CB2 1EZ, UK; fax: (+44)-1223-336-033; or e-mail: deposit@ccdc.cam.ac.uk).

Acknowledgements

We thank the EPSRC National Centre in Swansea for MS measurements; CITER for the MS facility in Cardiff; Syntex for funding C. C.'s Ph.D. studentship and Johnson Matthey for a generous loan of IrCl_3 . Dr. Ian A. Fallis (Cardiff University) is also gratefully acknowledged for useful discussions during the preparation of this manuscript and Mr. Robert L. Jenkins for assistance with the NMR measurements.

References and Notes

- [1] a) S. Vargas, M. Rubio, A. Suarez, A. Pizzano, *Tetrahedron Lett.* **2005**, *46*, 2049–2052; b) P. Maire, S. Deblon, F. Breher, J. Geier, C. Bohler, H. Ruegger, H. Schonberg, H. Grutzmacher, *Chem. Eur. J.* **2004**, *10*, 4198–4205; c) C. Blanc, F. Agbossou-Niedercorna, G. Nowogrocki, *Tetrahedron: Asymmetry* **2004**, *15*, 2159–2163; d) K. Fujita, T. Fujii, R. Yamaguchi, *Org. Lett.* **2004**, *6*, 3525–3528; e) A. Trifonova, J. S. Diesen, C. J. Chapman, P. G. Andersson, *Org. Lett.* **2004**, *6*, 3825–3827; f) W. B. Wang, S. M. Lu, P. Y. Yang, X. W. Han, Y. G. Zhou, *J. Am. Chem. Soc.* **2003**, *125*, 10536–10537; g) M. T. Reetz, T. Sell, R. Goddard, *Chimia* **2003**, *57*, 290–292; h) X. B. Jiang, A. J. Minnaard, B. Hessen, B. N. Feringa, A. L. L. Duchateau, J. G. O. Andrien, J. A. F. Boogers, J. G. de Vries, *Org. Lett.* **2003**, *5*, 1503–1506; i) Y. Chi, Y.-G. Zhou, X. Zhang, *J. Org. Chem.* **2003**, *68*, 4120–4122; j) D. Xiao, X. Zhang, *Angew. Chem. Int. Ed.*, **2001**, *40*, 3425–3428; k) A. Martorell, C. Claver, E. Fernandez, *Inorg. Chem. Commun.* **2000**, *3*, 132–135; l) K. Satoh, M. Inenaga, K. Kanai, *Tetrahedron: Asymmetry* **1998**, *9*, 2657–2662; m) P. Schnider, G. Koch, R. Prétôt, G. Wang, F. M. Bohnen, C. Krüger, A. Pfaltz, *Chem. Eur. J.* **1997**, *3*, 887–892; n) K. Tani, J. Onouchi, T. Yamagata, Y. Kataoka, *Chem. Lett.* **1995**, *10*, 955–956.
- [2] a) C. J. Copley, J. P. Henschke, *Adv. Synth. Catal.* **2003**, *345*, 195–201; b) S. M. Joseph Samec, J.-E. Bäckvall,

- Chem. Eur. J.* **2002**, *8*, 2955–2961; c) N. Uematsu, A. Fujii, S. Hashiguchi, T. Ikariya, R. Noyori, *J. Am. Chem. Soc.* **1996**, *118*, 4916–4917; d) J. Mao, D. C. Baker, *Org. Lett.* **1999**, *1*, 841–843.
- [3] a) Y. Chi, Y.-G. Zhou, X. Zhang, *J. Org. Chem.* **2003**, *68*, 4120–4122; b) V. Herrera, B. Muñoz, V. Landaeta, N. Canudas, *J. Mol. Catal. A: Chem.* **2001**, *174*, 141–149.
- [4] a) S. P. Smidt, N. Zimmermann, M. Studer, A. Pfaltz, *Chem. Eur. J.* **2004**, *10*, 4685–4693; b) A. Pfaltz, J. Blankenstein, R. Hilgraf, E. Hormann, S. McIntyre, F. Menges, M. Schonleber, S. P. Smidt, B. Wustenberg, N. Zimmermann, *Adv. Synth. Catal.* **2003**, *345*, 33–43; c) G. P. Xu, S. R. Gilbertson, *Tetrahedron Lett.* **2003**, *44*, 953–955; d) F. Menges, A. Pfaltz, *Adv. Synth. Catal.* **2002**, *344*, 40–44; e) D. G. Blackmond, A. Lightfoot, A. Pfaltz, T. Rosner, P. Schnider, N. Zimmermann, *Chirality*, **2000**, *12*, 442–449.
- [5] a) H.-U. Blaser, W. Brieden, B. Pugin, F. Spindler, M. Studer, A. Togni, *Top. Catal.* **2002**, *19*, 3–16; b) H.-U. Blaser, F. Spindler, *Top. Catal.* **1997**, *4*, 275–282.
- [6] H.-U. Blaser, H.-P. Buser, R. Häusel, H.-P. Jalett, F. Spindler, *J. Organomet. Chem.* **2001**, *621*, 34–38.
- [7] C. Carcedo, A. Dervisi, I. A. Fallis, Liling Ooi, K. M. A. Malik, *Chem. Commun.* **2004**, 1236–1237.
- [8] L. J. Farrugia, *J. Appl. Cryst.* **1997**, *30*, 565.
- [9] C. Carcedo, A. Dervisi, unpublished results.
- [10] a) M. T. Reetz, E. W. Beuttenmüller, R. Goddard, M. Pastó, *Tetrahedron Lett.* **1999**, *40*, 4977–4980; b) R. B. Bedford, P. A. Chaloner, P. B. Hitchcock, G. Lopez, F. Momblona, J. L. Serrano, *An. Quim.* **1996**, *92*, 354.
- [11] a) P. A. Chaloner, P. B. Hitchcock, M. Resinger, *Acta Crystallogr., Sect. C: Cryst. Struct. Commun.* **1992**, *48*, 735; b) R. B. Bedford, P. A. Chaloner, P. B. Hitchcock, *Acta Crystallogr. Sect. C: Cryst. Struct. Commun.* **1993**, *49*, 1614.
- [12] The largest bite angle observed within the dppm complexes is 103.52(9)° for Pt(dppm)Cl₂; unpublished results.
- [13] a) R. Dorta, D. Brogini, R. Stoop, H. Ruegger, F. Spindler, A. Togni, *Chem. Eur. J.* **2004**, *10*, 267–278; b) R. Sablong, J. A. Osborn, *Tetrahedron: Asymmetry* **1996**, *7*, 3059–3062.
- [14] J. P. Cahill, A. P. Lightfoot, R. Goddard, J. Rust, P. J. Guiry, *Tetrahedron: Asymmetry* **1998**, *9*, 4307–4312.
- [15] a) T. Sturm, W. Weissensteiner, F. Spindler, K. Mereiter, A. M. López-Agenjo, B. R. Manzano, F. A. Jalón, *Organometallics* **2002**, *21*, 1766–1774; b) G. X. Zhu, X. M. Zhang, *Tetrahedron: Asymmetry* **1998**, *9*, 2415–2418.
- [16] R. Dorta, D. Brogini, R. Kissner, A. Togni, *Chem. Eur. J.* **2004**, *10*, 4546–4555.
- [17] a) S. P. Smidt, A. Pfaltz, E. Martínez-Viviente, P. S. Pregosin, A. Albinati, *Organometallics* **2003**, *22*, 1000–1009; b) H. H. Wang, A. L. Cassalnuovo, B. J. Johnson, A. M. Mueting, L. H. Pignolet, *Inorg. Chem.* **1988**, *27*, 325–331; c) A. L. Casalnuovo, L. H. Pignolet, J. W. A. van der Velden, J. J. Bour, J. J. Steggerda, *J. Am. Chem. Soc.* **1983**, *105*, 5957–5958; d) H. H. Wang, L. H. Pignolet, *Inorg. Chem.* **1980**, *19*, 1470–1480; e) D. F. Chodos, R. H. Crabtree, *J. Organomet. Chem.* **1978**, *161*, C67–C70; f) R. H. Crabtree, H. Felkin, G. E. Morris, T. J. King, J. A. Richards, *J. Organomet. Chem.* **1976**, *113*, C7–C9.
- [18] K. Tani, A. Iseki, T. Yamagata, *Angew. Chem. Int. Ed.* **1998**, *37*, 3381–3383.
- [19] a) M. A. Esteruelas, M. P. Garcia, F. J. Lahoz, M. Martin, J. Modrego, E. Oflate, L. A. Oro, *Inorg. Chem.* **1994**, *33*, 3473–3480; b) J. D. Feldman, J. C. Peters, T. D. Tilley, *Organometallics* **2002**, *21*, 4050–4064.
- [20] dppp = 1,3-bis(diphenylphosphino)propane.
- [21] D. D. Perrin, W. F. A. Amarego, *Purification of Laboratory Chemicals*, Pergamon, Oxford, **1988**.
- [22] J. L. Herde, J. C. Lambert, C. V. Senoff, *Inorg. Synth.* **1974**, *15*, 18.
- [23] V. Cere, C. Paolucci, S. Pollicino, E. Sandri, A. Fava, *Tetrahedron Lett.* **1989**, *30*, 6737–6740.
- [24] B. C. Ranu, A. Majee, A. Sarkar, *J. Org. Chem.* **1998**, *63*, 370–373.
- [25] P. T. Beurskens, G. Beurskens, W. P. Bosman, R. de Gelder, S. Garcia-Granda, R. O. Gould, R. Israel and J. M. M. Smits, DIRDIF99.2 program system, Crystallography Laboratory, University of Nijmegen, The Netherlands, **1999**.
- [26] G. M. Sheldrick, SHELX97 [Includes SHELXS97, SHELXL97, CIFTAB (and SHELXA?)] – Programs for Crystal Structure Analysis (Release 97–2), Institut für Anorganische Chemie der Universität, Tammanstrasse 4, 3400 Göttingen, Germany, **1998**.
- [27] R. H. Blessing, SORTAV – Absorption correction, *Acta Crystallogr., Sect. A* **1995**, *51*, 33–38.